

Smart materials for active noise and vibration reduction

H. P. Monner

German Aerospace Center (DLR), Institute of Composite Structures and Adaptive Systems

Lilienthalplatz 7, D-38108 Brunswick, Germany

Abstract

For active noise and vibration reduction tasks in smart-structures technology piezoelectric ceramics are first choice. They generate large forces, have fast response times, are commercially available as fibres, patches and stacks and allow integration into structural components. Other commercialized smart materials are magnetostrictives and electrostrictives which have by far not reached the popularity of piezoelectric ceramics. However, the major limitation of these materials is their low actuator stroke. Therefore, in the past decade much effort has been made to generate new materials with larger strain rates. Especially the field of electroactive polymers has lead to the development of a considerable amount of promising materials which are able to perform very large active strains. Also the ferromagnetic shape memory alloys recently discovered are capable of generating large actuator strokes. However, also these new materials have their limitations. Especially their low mechanical stiffness presently only allows to produce comparably low forces. Thus, this article gives an overview of commercially available and emerging smart materials with special focus on active noise and vibration reduction tasks.

1 Introduction

Numerous applications of smart-structures technology are evolving to actively control vibrations, noise, and deformations. Applications range from space systems to fixed-wing and rotary-wing aircraft, automotive, optical systems, machine tools, medical systems, and infrastructure. A smart structure involves five key elements: structural material, distributed actuators and sensors, control strategies, and power conditioning electronics. With these components a smart structure has the capability to respond to changing environmental and operational conditions (such as vibrations and shape change). Microprocessors analyze the responses of the sensors and use integrated control algorithms to command the actuators to apply localized strains/displacements/damping to alter the elasto-mechanical system response. Actuators and sensors are highly integrated into the structure by surface bonding or embedding without causing any significant changes in the mass or structural stiffness of the system. In order to do so a fundamental part of smart structures are solid state actuators and sensors based on smart materials.

2 Smart materials

Especially due to the increasing demand in smart structures-technology smart materials have continuously been gaining attention in the past decade, although the physical effects of many typical candidate materials are known since over 50 years. These materials have the characteristic that they show both sensor and actuator effects. All these materials are capable of reversibly changing their mechanical properties (viscosity, stiffness, shape) due to the influence of temperature

change or an electrical or magnetical field. By some of these materials the reverse effect can be used for sensor tasks meaning that a mechanical load generates an electrical or magnetical field. Well-known are piezoelectric ceramics, magnetostrictive materials, and shape memory alloys.

Key issue for smart materials is the actuator performance. The limit of the actuator authority over the structure naturally marks the performance limit of the complete smart structure. Thus, this article gives an overview of smart materials with special focus on their actuator performance (active strain, forces, dynamics, energy density, ...) and their advantages and disadvantages for active noise and vibration reduction.

However, a tremendous variation in data concerning the mechanical and active properties of smart materials can be observed in literature and is provided by the different manufacturers. Partially the values differ between 100-200% or sometimes even more! This is mainly due to the large amount of possible compositions of the different smart materials. But also the variations within the manufacturing process itself are remarkable. E.g. experiments with shape memory alloys and piezoelectric ceramics have shown that the mechanical and active performance of the same material from the same manufacturer can differ 10-20%. Additionally the test procedures for characterizing smart materials are not standardized and also not published together with the available data. That is why all data presented within this article has to be seen as a starting point for estimating the performance of the different smart materials. It was tried to give an overview of the average performance values and not the theoretical maximum ones. When coming to the realization of a smart structure close cooperation with the manufacturers and eventually own characterization is strongly recommended.

2.1 Fundamental characteristics

Smart materials can be described by two key parameters: free strain ε_0 and blocking stress σ_B . The linear behaviour of a solid state actuator can be seen in the stress-strain diagram of Figure 1. Additionally a constant stress ($Y_s \cdot \varepsilon_s$) of a surrounding structure has been integrated into the diagram. The working point of an actuator is characterized by the intersection point between the characteristic lines of actuator and structure.

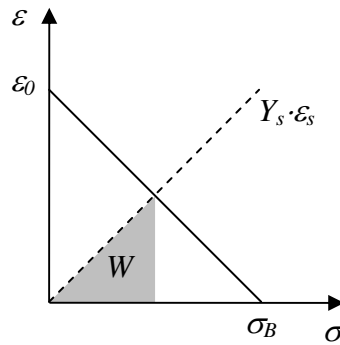


Figure 1: Stress-strain characteristic of a smart material

With the Young's modulus Y_a of the actuator the blocking stress can be written as

$$\sigma_B = Y_a \varepsilon_0. \quad (1)$$

The maximum volumetric work per cycle $W_{\max, \text{volumetric}}$ then is

$$W_{\max, \text{volumetric}} = \frac{1}{8} \sigma_B \varepsilon_0 = \frac{1}{8} Y_a \varepsilon_0^2. \quad (2)$$

The maximum gravimetric work per cycle can be calculated with the density ρ_a of the smart material

$$W_{\max, \text{gravimetric}} = \frac{W_{\max, \text{volumetric}}}{\rho_a} = \frac{1}{8} \frac{Y_a \varepsilon_0^2}{\rho_a}. \quad (3)$$

The volumetric work per cycle, also referred to as mechanical energy density, has to be considered to be of fundamental importance when comparing smart materials. Equation (2) represents the maximum energy that can be transferred to the mechanical structure by minimal actuator volume which is the case when the stiffness of the smart material is identical to the stiffness of the structural material. This means the actuator stress has to be $\sigma = \sigma_B/2$ and the actuator strain $\varepsilon = \varepsilon_0/2$. Impedance matching between smart material and structure is therefore basis for an efficient design.

2.2 Piezoelectric ceramics

Piezoelectricity was discovered 1880 by the brothers Pierre and Jaques Curie. A major breakthrough came with the discovery of lead zirconate titanate (PZT) in the 1950s. PZT exhibits very high dielectric and piezoelectric properties. Furthermore, it offers the possibility of tailoring their behaviour to specific responses and applications by the use of dopants. So far PZT is probably the most widely used piezoelectric material [1]. It can be differentiated between the direct and converse piezoelectric effect, which both are of constant volume on a macroscopic level. The direct piezoelectric effect produces a voltage when the material is strained whereas the converse piezoelectric effect causes a solid to become strained when placed in an electric field. Thus, piezoelectric ceramics can both be used as sensor and actuator. Piezoelectric ceramics are polycrystalline in nature and do not have piezoelectric characteristics in their original state. Piezoelectric effects are induced in these materials through poling beneath the Curie temperature at high dc electrical fields of ca. 2 kV/mm. This leads to an alignment of the polar axis of unit cells parallel to the applied field which results in a permanent polarization. Additionally, the ceramic is permanently mechanically deformed due to the reorientation of domains. Again, it has to be differentiated between the longitudinal, transversal and shear effect. The longitudinal effect describes the active strain in the polarization direction and parallel to the electric field, the transversal effect is the resulting Poisson strain in plane. The shear strain is generated parallel to the polarization direction and vertical to the electric field. Technical mainly the longitudinal and transversal effects are being used. The maximum strain of PZT is relatively small (0.12 - 0.18%) and is limited by saturation effects and depolarization [2]. Technically about 0.1% are used at 1 kV/mm and frequencies up to 100 kHz. PZT exhibits hysteresis of 2% for very small signals and reaches 10-15% at nominal voltage [3]. The density of PZT typically is about 7.6 g/cm³ [4]. Due to polarization PZT is not only electrical but also mechanical anisotropic. This means in longitudinal direction the Young's modulus is about 30% smaller than in transversal direction. For PZT the Young's modulus typically is about 50-70 GPa in longitudinal direction [5]. The piezoelectric effect itself also depends on the temperature. In the range <260 K, the effect decreases with falling temperature with a factor of approximately 0.4% per Kelvin. In the region of liquid nitrogen (ca. 77 K), the expansion due to the piezoelectric effect will be around 10–30% of the expansion at room temperature [6]. The upper temperature is limited by the Curie temperature. PZT actuators can reliably be driven up to 70% of the Curie temperature which lies between 150-350°C [5]. Temperatures above the Curie temperature cause depolarization. High mechanical stress can depolarize a piezoelectric ceramic, too. The limit on the applied stress should not exceed 20-30% of the mechanical compression load limit (200-300 MPa) [7]. Depolarisation also occurs when applying an electrical voltage opposite to the polarization direction larger than the coercive voltage. Piezoelectric ceramics are used in the form of thin sheets or fibers/stripes that can be attached or

embedded in composite structures or stacked to form discrete piezostack actuators (see Figure 2) and are the most popular smart material when it comes to active noise and vibration reduction tasks.

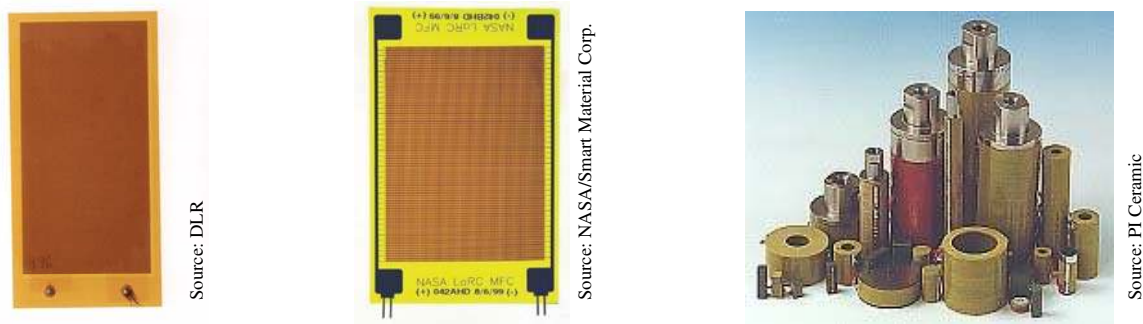


Figure 2: Available types of piezoceramic actuators - (a) Patch actuator, (b) Macro Fiber Composite (MFC) actuator, (c) Stack actuators

2.3 Piezoelectric polymers

Pioneering work in the area of piezoelectric polymers by Kawai [8] in 1969 has led to the development of strong piezoelectric activity in polyvinylidene fluoride (PVDF) and its copolymers with trifluoroethylene (TrFE) and tetrafluoroethylene (TFE). These semicrystalline fluoropolymers represent the state of the art in piezoelectric polymers and are currently the only commercially available piezoelectric polymers [9]. Phenomenological PVDF is similar to PZT. It can be differentiated between the direct and conversion effect (both of constant volume on macroscopic level) meaning it can be used as sensor and actuator. The electro-mechanical material behaviour shows longitudinal, transversal and shear effects whereas technically mainly the transversal effect is being used. However, there is one significant difference between PVDF and PZT concerning the electro-mechanical material behaviour: The piezoelectric strain constants (d_{31} , d_{32} , d_{33}) are of opposite sign. This means in direction of the electric field PVDF contracts instead of elongating like PZT. In plane PVDF elongates whereas PZT contracts. PZT has 10-20 times larger piezoelectric strain constants than PVDF [5, 10]. The active strain with 0.1% at up to 100 kHz is in the order of magnitude of PZT but requires significant larger electrical fields of 10-20 kV/mm. In order to render PVDF piezoelectric, it must have a polar crystalline phase. PVDF consist of crystallites dispersed within amorphous regions. The amorphous region has a glass transition temperature ($\sim 40^\circ\text{C}$) that dictates the mechanical properties of the polymer while the crystallites have a melting temperature ($\sim 180^\circ\text{C}$) that dictates the upper limit of the use temperature. However, the piezoelectric effect is limited by the Curie temperature ($\sim 100^\circ\text{C}$). Reliably PVDF can be used at a maximum temperature of about $60\text{-}80^\circ\text{C}$ [11, 12]. The degree of crystallinity present in such polymers depends on their method of preparation and thermal history. Mechanical orientation, thermal annealing and high voltage treatment have all been shown to be effective in inducing crystalline phase transformations. Stretching the polymer essentially aligns the amorphous strands in the film plane and facilitates uniform rotation of the crystallites by an electric field. Electrical poling is accomplished by applying an electric field across the thickness of the polymer. An electric field on the order of $50\text{-}80\text{ kV/mm}$ is typically sufficient to effect crystalline orientation. Depending on whether stretching is uniaxial or biaxial, the electrical and mechanical properties are either highly anisotropic or isotropic in the plane of the polymer sheet. In plane the Young's modulus varies between $2\text{-}3\text{ GPa}$. In direction of the electric field the Young's modulus is about 1 GPa [10]. In stretching direction the Young's modulus is lower than vertical to it. The piezoelectric strain constants on the other hand are larger in stretching direction. Similar to PZT care must be taken to

avoid applying too large voltage, mechanical stress, or temperature for fear of depoling the material. Advantage of PVDF over PZT is the low density of about 1.47 g/cm^3 [10] and the processing flexibility because tough, readily manufactured into large areas, and can be cut and formed into complex shapes. Major disadvantage is their low stiffness significantly reducing authority over the structure limiting PVDF to applications with low requirements concerning the forces.

2.4 Electrostrictive ceramics

Electrostriction is a general term referring to the elastic deformation of a dielectric material under the influence of an electric field. Strictly speaking, PZT therefore also belongs to the category of electrostrictive ceramics since electrostriction exist in almost all materials but is usually very small in effect. In a narrower sense, however, the term ‘electrostrictive ceramics’ is used to describe ceramics such as those based on lead magnesium niobate (PMN) that, in contrast to piezoelectric ceramics, are not polarized but rather exhibit a change in length due to a spontaneous orientation of dipoles in an electric field. In contrast to piezoelectric ceramics, electrostrictive ceramics elongate in the presence of both positive and negative electric fields. The resulting strain is proportional to the square of the electric field. Without electrical field electrostrictives are isotropic, with electric field ($\sim 1.3 \text{ kV/mm}$) the transverse material stiffness decreases by about 20%. The actuation forces and frequencies as well as the required electrical fields are comparable to those of PZT. The strain, however, is about 10-20% smaller and the hysteresis with ca. 1-3% much less. Electrostrictive materials like PMN used to date are much more temperature-sensitive than piezoelectric ceramics, and their operation temperature is less than 40°C [4, 11, 13]. Electrostrictive ceramics are of less practical importance than piezoelectric ceramics due to their temperature dependence.

2.5 Magnetostrictive materials

The magnetostrictive effect was discovered 1842 by James Prescott Joule first in nickel. In the following years other materials like cobalt, iron and their alloys were shown to have magnetostrictive effects like nickel. The maximum strains reached were about 0.005%. Beginning of 1970 a research group at Naval Ordnance Lab (NOL) discovered Terfenol-D, which produced a significantly larger magnetostriction resulting in a maximum strain of the order of 0.1-0.2%. Practical strains employed by the manufacturers of Terfenol-D actuators are in the quasi-linear behaviour range of 0.075-0.1 %. Eddy currents lead to the frequency limitation (max. 10 kHz) of bulk Terfenol-D [15]. Terfenol-D consists of iron and the rare earth elements terbium and dysprosium and is normally available in the form of rods of different diameters. With no magnetic field oblong magnetic domains in the material are randomly oriented. When compression stress is applied, most of the domains get oriented normal to rod’s axis. In the presence of a magnetic field along the longitudinal axis these domains rotate and become mostly parallel to this longitudinal axis and induce extensional strain. If the magnetic field is reversed, the domains reverse direction, but again induce an extensional strain. This magnetostrictive effect is of constant volume on a macroscopic level, meaning that the diameter shrinks as a result of Poisson’s effect. The strain increases quadratically with magnetic field intensity H . The magnetic field intensity H typically is in the region of 50-200 kA/m (625-2500 Oe). Besides the Joule effect similar to the piezoelectric materials a reciprocal effect exists, which is called Villari effect. An application of stress, causing the material to strain, results in a change in its magnetic field. The Joule effect is used for actuators, whereas the Villari effect is used in sensors. The Young’s modulus is strongly dependent on the magnetic field and the applied compressive stress and can vary between 25-65 GPa [14, 15]. Terfenol-D has a density of $9.15\text{-}9.25 \text{ g/cm}^3$ [15]. The Curie temperature is about 380°C . When

heating Terfenol-D beyond this temperature the magnetostrictive effect is not permanently eliminated and returns after operating beneath Curie temperature again. However, at high operating regimes hysteresis and nonlinearities are intrinsic to magnetostrictive behaviour. The magnetic field is produced either by a magnetic coil surrounding the rod or by a permanent magnet. Most commonly a configuration is chosen where a permanent magnet is used to generate a steady bias field, and an ac current is applied to control the time-varying magnetic field or strain respectively. This type of configuration leads to 10-20 times heavier actuators in comparison to piezoceramic stack actuators (including the housing) [17]. This is also mainly the reason why in smart-structures technology preferable piezoceramic stack actuators are being used, though the performance of Terfenol-D itself is partially better than PZT. However, meanwhile Terfenol-D is available in form of thin films probably enabling new types of smart structures.

2.6 Shape memory alloy (SMA)

First investigations related to the shape memory effect were reported by A. Ölander. He discovered the pseudoelastic behaviour of the Au-Cd alloy in 1932 [18]. In 1961, the U.S. Naval Ordnance Laboratory discovered the shape memory effect in a nickel-titanium alloy which then was named Nitinol (Nickel-Titanium Naval Ordnance Laboratory). Nitinol can be considered a breakthrough in the field of shape memory materials because it exhibits much higher shape memory effects than previous materials [19]. SMAs have two stable phases - the high-temperature phase, called austenite and the low-temperature phase, called martensite. The austenite crystal structure is a simple cubic structure with only one possible parent phase, while martensite has a more complex rhombic structure with a total of 24 crystallographically equivalent habit planes. This phenomenon causes the SMAs to revert completely to the shape it had before the deformation. While NiTi is soft and easily deformable due to de-twinning in its lower temperature form (martensite), it resumes its original shape and rigidity when heated to its higher temperature form (austenite). This is called the one-way shape memory effect allowing 100% strain recovery of up to a maximum of 8% extensional prestrain. The ability of shape memory alloys to recover a preset shape upon heating above the transformation temperatures and to return to a certain alternate shape upon cooling is known as the two-way shape memory effect. This requires special training of the shape memory alloy. Training typically consists of several cycles of deformation to the desired low-temperature shape and subsequent shape recovery [20]. It is possible to train the NiTi alloy in different ways: Extension, compression, or shear are deformations that can be reversed by heating. In applications mainly the extension training is being used. The usable two way strain is strongly dependent on the requirements concerning amount of cycles and the stress/strain mode. The following Table 1 presented by Memory-Metalle GmbH [21] is a guideline for standard binary NiTi alloys. However, special treatment of the NiTi alloy may result in longer lifetime.

Cycles	Max. strain [%]
up to 1	8
up to 100	5
up to 100,000	3
above 100,000	2

Table 1: Recoverable strain as a function of the number of cycles for NiTi

Above the transition temperature, shape memory alloys show an extraordinary elasticity of 6-8 % reversible strain which is far beyond that of conventional materials. The restoring force is nearly independent of the strain. This effect is referred to as superelasticity and is based on stress-induced

martensite formation. NiTi alloys are available as wires, rods, tubes, ribbons, and thin sheets. The Young's modulus for martensite is 21-69 GPa and austenite 70-110 GPa [22] meaning austenite has a two- to fourfold larger Young's modulus in comparison to martensite. Operating frequencies in the two-way mode typically are <1 Hz because cooling of the materials is a rather slow process. SMAs can be activated by external heating (SMA reacts to the ambient temperature) or electrical heating (Joule heating with electrical current). By electrical heating the energy consumption carefully has to be considered since most of the input energy is transformed to heat rather than mechanical strain resulting in low efficiency (<2 %). NiTi alloys have a density of about 6.45 g/cm³ [21]. The transformation temperature between low-temperature and high-temperature phase (-200 to +110°C) [21] can be adjusted by varying the proportions between nickel and titanium within the alloy. Due to their slow response time and low efficiency active noise and vibration reduction tasks are not the domain of NiTi alloys. However, by using the hysteresis of the superelastic effect for structural damping or changing the eigenfrequencies by generating internal compressive stress in a structure for certain specialised applications SMAs can be an interesting alternative.

3 Emerging smart materials

3.1 Ferromagnetic shape memory alloys (FSMAs)

The effect was first described by K. Ullakko in 1996 [23]. Ferromagnetic shape memory alloys (FSMAs) consisting of Ni-Mn-Ga alloys have been shown to produce large strains of 6-10% when exposed to magnetic fields of 400 - 640 kA/m (5000-8000 Oe) [24, 25]. Actuators systems with FSMAs typically achieve 2-3 % active strain [25]. These strains result from the reorientation of twinned martensitic variants and associated twin boundary motion which occur as the easy crystallographic axis aligns with external magnetic fields (see Figure 3(a)). While these strains are on the same order of those seen in shape memory alloys, the rotation of twin martensitic variants in response to magnetic activation is faster and thus can lead to faster response than those achieved through martensite-austenite phase transformations [26].

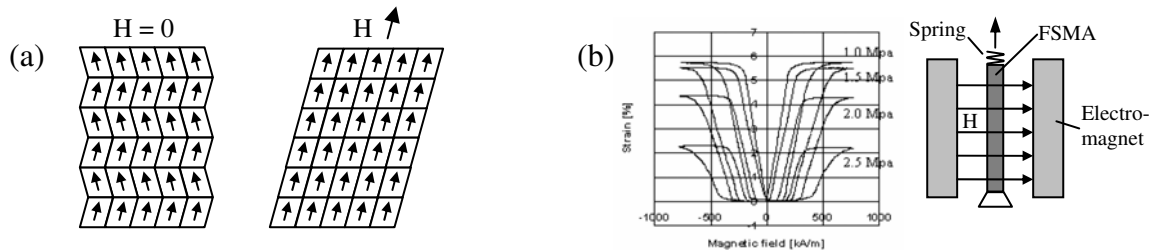


Figure 3 : (a) Principle of magnetic field induced re-orientation of martensitic variants,
(b) Magnetic-field-induced strains vs. magnetic [26]

Upon removal of the external magnetic field, however, there is no restoring force to drive the twin boundary in the opposite direction and the field-induced strain is not recoverable. FSMA material can generate its shape change in different modes: axial, bending, or torsion motion. However, commonly only the linear axial motion is of practical use [25]. To achieve large reversible field-induced strains, a compressive stress is typically applied perpendicular to the field direction (see Figure 3(b)). Optimal compression load to reach maximal magnetic-field-induced strain is about 1 - 1.5 MPa [25]. Ni-Mn-Ga alloys have a field and strain dependent Young's modulus of 0.45 - 0.82 GPa [27]. The density of the material is 8.36 g/cm³ [27]. Operating temperatures of Ni-Mn-Ga MSM materials presently range from -40°C to 60°C. Rise time is less than 0.2 ms and theoretically allows to drive a FSMA actuator at a many kHz. However, flux generation, the natural frequency of

FSMA and the inertia of the moving mass often limit the operating frequency to a few 100 Hz. It can be expected that the material properties will further improve making this material an interesting and considerable material in future active noise and vibration reduction tasks.

3.2 Electroactive polymers

The effect of electroactive polymers (EAPs) was first investigated by Wilhelm Conrad Roentgen in 1880. In an experiment using 16×100 cm strips of natural rubber with a fixed mass attached to the free end he was able to induce strain by charging and discharging the rubber [28]. Since the early 1990s many new polymers have emerged that respond to electrical stimulation with a significant shape or size change. EAP often are referred to as ‘Artificial Muscle’ since they behave similar to biological muscles. Basically, EAPs can be divided into two major categories based on their activation mechanism: electronic (driven by electric field or Coulomb forces) and ionic (requiring mobility or diffusion of ions). Electronic EAPs require high electric fields (~ 150 kV/mm), have fast response times and exhibit high mechanical energy density. Ionic EAPs can be driven at low voltage (1-10 V), have rather slow response times and require using an electrolyte. Following a selection of some promising EAP developments are presented. An extensive description of EAPs can be found in [29].

3.2.1 Electric EAPs

Electrostrictive Polymers

Besides the piezoelectric effect described in section 2.3 PVDF and its copolymers can also induce electrostrictive strains of 2% when applying large ac electric fields (200 kV/mm). However, this level of field is close to dielectric breakdown and the large dielectric hysteresis causes strong heating of the material. For this reason the piezoelectric in PVDF effect has been mainly investigated and commercialized. This might be changing since in 1998 Zhang introduced defects into the crystalline structure using electron radiation to reduce dielectric loss dramatically in a PVDF-TrFE copolymer [30]. This results in much less heat generated in an ac electric field. Electrostrictive strains of up to -5% (parallel to the electric field) can be achieved at low-frequency driven fields with amplitudes of about 150 kV/mm. The Young’s modulus is about 1 GPa for this polymer and the field induced strain can be operated at frequencies beyond 100 kHz [29]. The strain is proportional to the square of the applied electric field. The density of this polymer is about 1.9 g/cm^3 [29]. It could be shown that the strain response does not change appreciably within a temperature range of 15-75°C. For stretched films it is possible to generate large transverse strain of about +4.5% along the stretching direction under an electric field of 85 kV/mm [31]. For unstretched films the transverse strain is relative small (+1% at 100 kV/mm) while the ratio between transverse and longitudinal strain is less than 0.33 [32]. Recent investigations show that a drastic reduction of the driving electric fields of electrostrictive polymers can be obtained by mixing a highly dielectric component with the polymer matrix. In particular, composite materials realized by using P(VDF-TrFE) as polymeric matrix and copper-phthalocyanine (CuPc), as organic filler with high dielectric permittivity, showed a 2% strain with an applied electric field of 13 kV/mm [33]. Considering the enormous active strains combined with high operation frequencies this type of EAP could be very interesting for various active noise and vibration reduction tasks. Drawback is the low stiffness of the polymer limiting it to applications with reduced force requirements.

Electrostrictive Graft Elastomers

NASA Langley research Center developed a grafted elastomer that generates high electrostrictive longitudinal strain ($\sim 4\%$) under large electric fields (~ 120 kV/mm) [34]. The strain exhibits a quadratic dependence with the applied electric field. These elastomers have been operated at 100-1000 Hz and have a density of about 1.78 g/cm³ [34]. This electrostrictive polymer consists of two components, a flexible macromolecule backbone and a grafted polymer that can be produced in a crystalline form. The flexible backbone polymer studied is a copolymer of chlorotrifluoroethylene and trifluoroethylene, while the grafted polar crystalline polymer is a copolymer of vinylidene-fluoride and trifluoroethylene, P(VDF-TrFE). The Young's modulus is about 0.55 GPa. Investigations show that 95% of the strain induced by the electric field is due to electrostriction, while the contribution from the Maxwell stress effect is less than 5%. Tests show that these actuators function at -50 to 100°C [34]. This EAP also can be seen as a very interesting material for active noise and reduction, especially since it is said to be easy to manufacture [34]. Similar to the electrostrictive polymers the low Young's modulus has to be considered in the structural design. Also the large electric fields required will be a challenging task when brought into application

Dielectric EAP

A dielectric EAP is also known as electrostatically stricted polymer (ESSP). A polymer with low elastic stiffness and high dielectric constant is positioned between two compliant electrodes. When an electric field is applied across the polymer film, the unlike charges on the opposing electrodes will attract each other and tend to squeeze the film in thickness and expand the film in transverse direction. The stress induced in the film is equal to the permittivity of the film multiplied by the permittivity of free space and the square of the electric (see Figure 4).

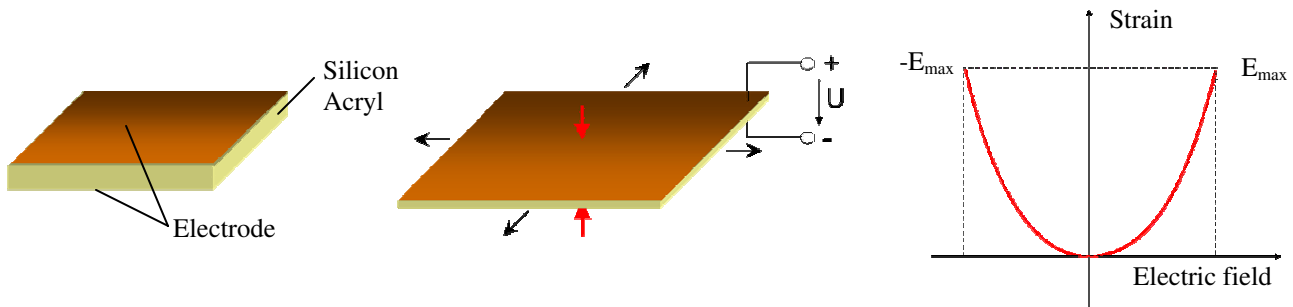


Figure 4: Deformation of elastomer (silicone, acryl) under an applied voltage

Two types of polymers are commonly used for dielectric EAP: an acrylic elastomer from 3M (VHB 4910) or silicone elastomer (PDMS – polydimethylsiloxane). The former has the better properties but it is only available as an adhesive tape that cannot be processed further, whereas two-component silicone elastomers are easily cast and moulded into any thickness and form. For example, the film and electrode can be formed into a tube, rolled into a scroll, stretched over a frame, or attached to a flexible structure to produce bending. Silicon materials from NuSil Corporation (NuSil CF19-2186) and Dow Corning Corporation (Dow Corning HS III) have shown to produce largest strain responses [29]. The density of these materials is 1.1 g/cm³ [35] and 1.16 g/cm³ [36], respectively. Compliant electrode materials typically include silicones or other polymers combined with carbon or other conductive particles. The Acrylic elastomer from 3M has a Young's modulus of 3 Mpa and has shown relative area strains up to 215% at an electric field of 240 kV/mm. The density of this material is listed with 0.8 g/cm³ [37]. The Silicon Materials NuSil CF19-2186 and Dow Corning HS III have a Young's modulus of 0.1 and 1.0 Mpa, respectively, and have produced relative area strains of 117% (at 128 kV/mm) and 63% (at 181 kV/mm), respectively [29]. The silicon material NuSil CF19-2186 is one of the best-performing dielectric elastomers and is known to exhibit stable mechanical properties over a fairly wide range of temperatures (-65°C to $+240^\circ\text{C}$) [38]. Other types of silicon rubber have shown operation temperatures below -100°C [38].

The Acrylic elastomer from 3M has been shown to operate over a range -10°C to $+80^{\circ}\text{C}$ [29]. However, it can not be expected that full performance can be sustained over the full temperature range [38]. The maximum driving frequencies are mainly limited by the natural frequency of the elastomer and the inertial load. E.g., the natural frequency of a 100 mm long acrylic actuator is about 120 Hz. From all EAPs this material seems to be most mature and closest to be commercialized. Due to their giant active strains for certain applications this material could be a very interesting candidate. Again here the very low Young's modulus has and the high driving voltages will be the key issues when coming to application.

3.2.2 Ionic EAPs

Ionomeric Polymer-Metal Composites (IPMC)

This type of bending actuation in a polymer was described by K. Oguro in 1992 [39]. A typical IPMC consists of a thin (200 μm) polymer membrane with metal electrodes (5-10 μm) plated on both faces and bends in response to an electrical activation as a result of the mobility of cations in the polymer network (see Figure 5).

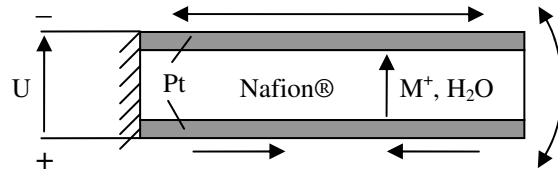


Figure 5 : Principle of an IPMC actuator

Two types of base polymers are employed to form IPMCs. These are Nafion® (perfluorosulphonate manufactured by Du Pont) and Flemion® (perfluorocaboxylate manufactured by Asahi Glass, Japan). In order to chemically electrode the polymer films, metal ions (platinum, gold or others) are dispersed throughout the hydrophilic regions of the polymer surface and are subsequently reduced to the corresponding zero-valence metal atoms. To maintain the actuation capability, the film needs to be kept moist continuously. IPMC require relatively low voltages to stimulate a bending response (1-3 V) with low frequencies below 1 Hz. The displacement significantly decreases with increase in frequency [40]. Typically IPMC can achieve deflections at the tip of about 7 % of the overall length of the sample [41] which corresponds to active strains of 2.3-2.6% [42]. The Young's modulus varies between 50 – 1500 Mpa and more due to a strong dependence on the presence or absence of solvent and the type of cations being used. Basically it can be stated that the dryer the sample is the larger the Young's modulus gets. The influence of the type of cation then gains, too. However, the Young's modulus for a wet IPMC actuator with Nafion® is 90-190 Mpa [43]. Due to their low operating frequencies and small Young's modulus this type of actuator presently seems to be of minor interest for active noise and vibration tasks.

Conductive Polymers (CP)

An EAP actuator of this type was first suggested by E. Smela in 1995 [44] consists of two layers of conductive polymer electrodes with an electrolyte between them. Conductive polymer electrodes are commonly fabricated from polypyrrole or polyaniline. CPs actuate via the reversible counter-ion insertion and expulsion that occurs during redox cycling. Significant volume changes occur through oxidation and reduction reactions at corresponding electrodes through exchanges of ions with an electrolyte. When a voltage is applied between the electrodes oxidation occurs at the anode and reduction at the cathode. Oxidation leads to a removal of ions causing shrinkage of the polymer and conversely addition of ions results in swelling [45] (see Figure 6).

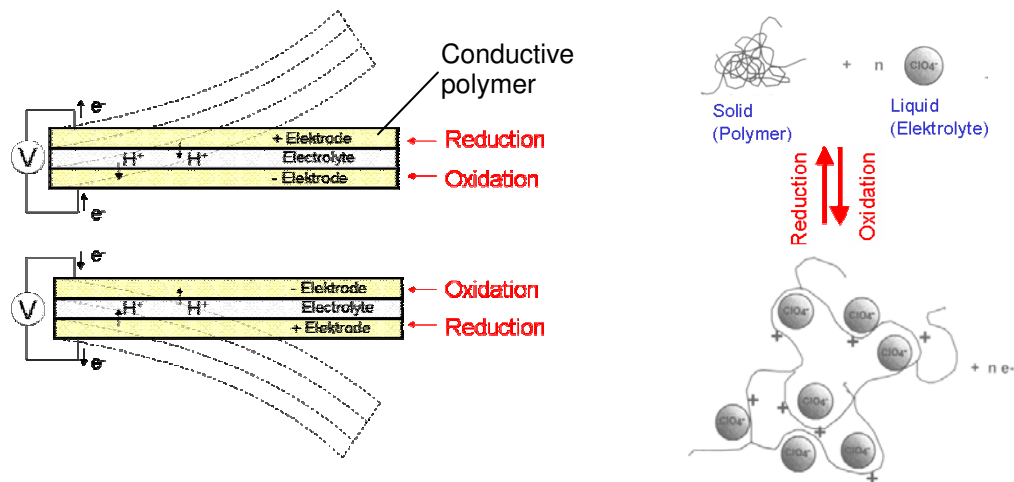


Figure 6: Activation mechanism of conductive polymer bending actuators [29]

Commonly CP actuators are used as bending beams. CP actuators require voltages in the range of 1-5 V. Variations to the voltage can control actuation speeds. Also the thickness of the CP layers influences the response speed. Thinner layers are faster but induce lower force. CP actuators typically exhibit active strains in the order of 1-10 % [46] and have a Young's modulus of about 1.4 GPa (polyanilin) [47]. The density of the CP polyanilin is about 1.5 g/cm³ [29]. In order to perform actuation maintaining of wetness is required. Strain rates vary between 0.1-3 %/s resulting in frequencies of about 0.05-1 Hz, whereas up to 30 Hz have been realized with reduced displacements [46]. CPs posses low efficiencies at levels of 1%. Presently the actuators lifetime still is reduced due to a delamination between the layers and degradation processes that occur in the CP layers [29]. Maximum lifetime reported is over 3·10⁵ cycles [47]. The progress made lately in increasing the materials stiffness and the response speed could make this actuator type an interesting candidate for certain low frequency active noise and vibration reduction tasks. However, the biggest challenge will be to develop CP actuators which function without a liquid electrolyte and use solid polymer electrolytes instead [29].

Carbon nanotubes actuator

Since they were first observed about a decade ago by S. Iijima [48], carbon nanotubes have been in the focus of considerable research. A carbon nanotube is a cylindrical shell built up of carbon atoms with a diameter as small as 1-20 nm and a length of up to 100 micrometers. It consists of pure covalently bonded carbon and can be pictorially described as a sheet of graphite that has been rolled into a tube. Nanotubes exist either as single-walled or multi-walled structures (see Figure 7 (a)). Multi-walled carbon nanotubes (MWNT) are composed of concentric single-walled nanotubes (SWNT). SWNTs show ideal mechanical properties, better than MWNTs since the transmission of low shearing stresses between the inner and outer MWNT walls reduces the possible stiffness and strength that are found in SWNTs. Small diameter SWNTs (~3 nm) are very stiff and exceptionally strong with a very high Young's modulus and high tensile strength. With the total area per nanotube in a nanotube bundle for normalising the applied force to obtain the applied stress, the calculated Young's modulus for an individual nanotube [49] is ~0.64 TPa, which is consistent with measurements [50]. Because small diameter nanotube ropes have been elastically extended by 5.8% before breaking, the SWNT tensile strength calculated from the product of this strain and modulus is ~37 GPa [50, 51]. The density of SWNTs is 1.33 g/cm³. In 1999 R. H. Baughman reported that SWNTs can also be used as electrochemical actuators which, when placed in an electrolyte, function at a level of just few volts and can generate up to ~1% extensional strain [52]. The activation mechanism is based on double-layer charge injection. Together with the quantum

chemical effects, this double layer of ions causes large dimensional changes in the covalent bonds of the nanotubes (see Figure 7 (b)).

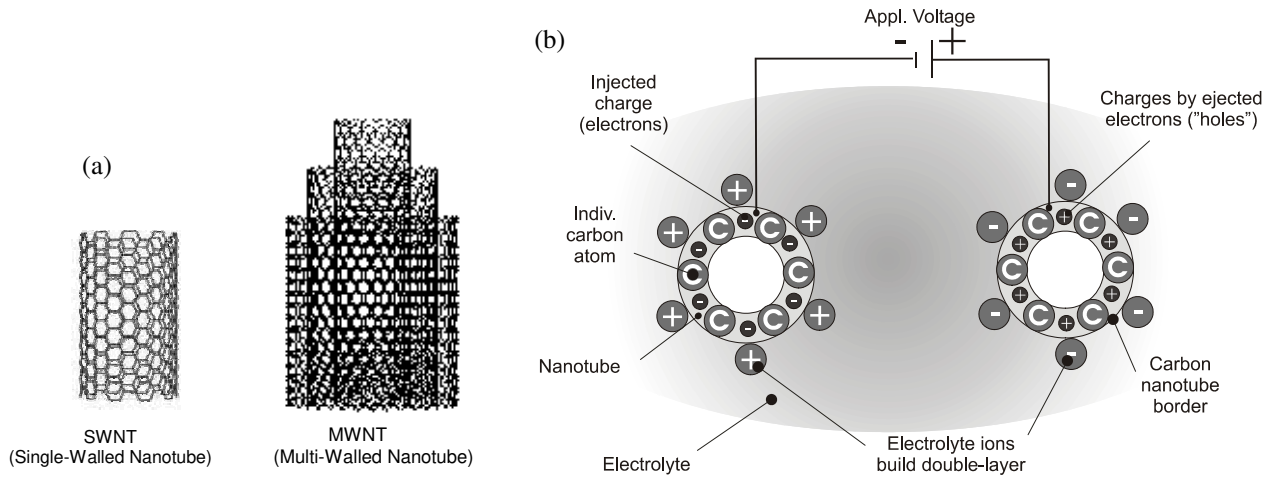


Figure 7: (a) Single-walled and multi-walled carbon nanotubes, (b) Principle of double-layer charge injection [52]

However, all these remarkable mechanical and actuatoric properties are based on the full performance of the single carbon nanotube. The challenge will be to achieve these properties of individual SWNTs also in macroscopic nanotube assemblies that are found in sheets and continuous fibres. Sheets available today with randomly distributed carbon nanotubes, also called “bucky paper“, have a maximum Young’s modulus of 0.3-6 Gpa [53]. Bucky paper is conventionally obtained by filtering SWNTs dispersed in a liquid, peeling the resulting sheet from the filter after washing and drying, and annealing the sheet at high temperatures to remove impurities. The SWNTs are only loosely connected by van der Waals forces. Used as actuator, bucky paper can generate strains of $>0.2\%$ [52]. Very promising are recent developments concerning carbon nanotube fibres that contain nearly 100% SWNTs. They are obtained by a coagulation-based process that enables continuous fibres to be spun with nanotube orientations of $\pm 10^\circ$ in regard to the fiber axis. Actuators based on carbon nanotube fibres generate an experimentally verified active strain of 0.5 to 1% [54]. A Young’s modulus of 80 Gpa and a failure strength of 1800 Mpa is reported for such fibres [55]. Since carbon nanotubes offer high thermal stability they eventually can be used at temperatures above 1000°C . Therefore, the surrounding electrolyte will be more critical concerning the operating temperature. Because nanotube actuation depends on ion diffusion the response time of a bucky paper specimen is about ~ 5 s resulting in frequencies of ~ 0.1 Hz, although respond could be observed at >1 kHz at significantly reduced strain levels [52]. As can be seen, presently the best mechanical and actuator properties reported for SWNTs in the form of carbon nanotube fibers and bucky papers are still significantly below the full performance of single SWNTs. One challenge is the improvement of mechanical properties of nanotube sheets and fibres with a high surface area (for double layer charging) by increasing the nanotube parallel alignment and the binding between the nanotubes without decreasing the actuator performance. Another challenge will be to find sufficient solid polymer electrolytes which provide good ionic conductivity without degrading the performance of the nanotubes [29]. In all, SWNT actuators are a very interesting candidate for active noise and vibration reduction tasks in the lower frequency range. Especially their large (theoretical) Young’s modulus promises exceptional stress performance in comparison to all other EAPs described.

4 Performance summary of smart materials

In the following Table 1 the performance of the different smart materials presented in this paper are summarized. Additionally, the volumetric work per cycle and gravimetric work per cycle has been calculated according to the equations (2) and (3), respectively.

Material	Young's modulus Y_a [Gpa]	Max actuator strain ε_0 [%]	Density ρ_a [g/cm ³]	Operating frequency at ε_0 [Hz]	Blocking stress σ_B [MPa]	Volumetric work per cycle (2) [J/cm ³]	Gravimetric work per cycle (3) [J/kg]
<i>"Classic" smart materials</i>							
PZT	50-70	0.12-0.18	7.6	100,000	72	0.0108	1.42
Terfenol-D	25-65	0.075-0.2	9.15-9.25	10,000	82.5	0.0155	1.67
PVDF	2.1-2.5	0.1	1.47	100,000	2.3	0.000288	0.196
NiTi	70-110 (a)	2-8	6.45	1	425*	1,59*	247*
<i>Emerging smart materials</i>							
FSMA	0.45-0.82	2-10	8.36	100-1,000	18	0.0675	8.1
PVDF-TrFE	1	2-4	1.9	100,000	40	0.2	105
ESSP-Silicon	0.0001-0.001	117-63	1.1-1.15	100-1000	0.63	0.0496	45
ESSP-Acrylic	0.003	215	0.8	10-100	6.45	1.733	2167
Grafted Polymers	0.55	4	1.78	100-1,000	42.6	0.11	62
CP-Polyanilin	1.42	1-10	1.5	0.1-1	22	0.16	106
IPMC-Nafion	0.09-0.19	2.3-2.6	2.5-2.9	1	4.75	0.0148	5.1
SWNT theory	640	1	1.33	1-10	6400	8	6015
SWNT fiber	80	0.5-1	1.33	0.1	400	0.25	188
SWNT sheet	0.3-6	0.2	1.33	0.1	10	0.0025	1.88

Table 2: Comparison of smart material properties

* The calculated blocking stress σ_B for the shape memory alloy NiTi exceeds the ultimate tensile strength of 1900 MPa [21]. Therefore, the average value of 425 MPa for the plateau stress of austenite (200-650 MPa) given by Memory Metalle GmbH was taken to calculate the volumetric work per cycle and gravimetric work per cycle.

5 Conclusions

Many promising new materials are emerging from the field of the electro active polymers. The field of EAPs is rather new and of course far from being mature. But the progress made in the past years and the increasing amount of research groups working on this field makes it seem only a matter of time until EAPs will find their way into numerous applications. For noise and vibration reduction tasks electric EAPs are advantageous since they have fast response times and generate large strain (up to 215%). However, field activated EAPs such as ESSP and PVDF-TrFE are highly capacitive loads. Further, the maximum electric fields of up to 150 kV/mm require typically quite high voltages to be applied. This combination presents challenges for the electronic driver circuits. Theoretically, a high electric field can be achieved at fairly low voltages by the use of thin films. In practice, such thin films are presently difficult to produce reliably in large areas, so most applications will employ thicker films that require voltages of several hundred to several thousands of volts. At present, small electronics that operate at voltages of several thousand volts, such as transistors and integrated circuits, are not available. However, there are no fundamental obstacles to the development of high voltage devices. The currently available selection reflects the existing market demand rather than technology limitations. When field-activated EAPs become more widespread the required electronic circuits will advance, too. So when large active strains and low forces at moderate (ESSPs) to high frequencies (PVDF-TrFE) are required these materials are a candidate to be first choice for certain applications in future. Especially the ESSPs are quite

matured. Silicon-based ESSP have been tested at 5 % strain to more than 10^7 cycles at 10 Hz without any observable degradation in performance [29]. From all EAPs this material seems to be closest to commercialization.

The ionic EAPs are not quite so matured as some of the electric EAPs. They offer large strains at moderate voltages (1-5 V) and operate presently at low frequencies. Main challenge is to optimize the ion exchange process since this directly influences the response times. Key element is the electrolyte which can either be an electrolyte solution or a dry/wet polymer electrolyte. When using a liquid medium the ionic EAPs have to be encapsulated. The problem is to find a good encapsulating material whose mechanical stiffness does not reduce the actuators performance. If a solid polymer electrolyte (e.g. Nafion®) is utilized, no encapsulating material is needed. However, ionic conductivity is lower than in liquid electrolytes which is an important problem that has to be resolved. Progress also still has to be made when it comes to durability tasks. Ionic EAPs presently have a relative short lifetime. Though far from application, especially the carbon nanotube actuators are of special interest since they have theoretically the capability to generate both large strains and large forces.

FSMAs offer as one promising non-EAP material large strains, small forces and moderate response times. They are relative matured and are already commercially available from Adaptamat. Further improvement of the materials properties can be expected making this material an interesting candidate for certain active noise and vibration reduction tasks. However, it has to be considered that large magnetic fields are needed which require relative heavy and voluminous electromagnets.

Though all of these promising materials are emerging piezoelectric ceramics still will be first choice when it comes to active noise and vibration reduction tasks in the high-force and/or high-frequency region, though they have their limitations in actuator stroke. For special requirements (hysteresis, temperature, active strain) magnetostrictives and electrostrictives are presently the only alternatives. This is presently a fact that one has to cope with.

6 References

- [1] T.L. Jordan, Z. Ounaies, 'Piezoelectric Ceramics Characterization', NASA/CR-2001-211225, ICASE Report No. 2001-28 (2001)
- [2] A. Schönecker, B. Brückner, T. Rödig, S. Gebhardt, 'Piezoaktuatorik für Adaptronik-Komponenten', Chemnitzer Produktionstechnisches Kolloquium (CPK), Chemnitz, Germany (1994)
- [3] http://www.piceramic.com/pdf/PIC_Tutorial.pdf
- [4] V. Giurgiutiu, R. Pomirleanu, C. A. Rogers, 'Energy-Based Comparison of Solid-State Actuators', University of South Carolina, Report # USC-ME-LAMSS-2000-102, March 1, 2000
- [5] <http://www.piceramic.com/pdf/material.pdf>
- [6] http://www.piezojena.com/img_db/dl_mg_1040388237.pdf
- [7] <http://www.physikinstrumente.de/products/prdetail.php?secid=4-23>

- [8] H. Kawai, 'The Piezoelectricity of Poly(vinylidene fluoride)', Jpn. J. Appl. Phys., **8**, p. 975, (1969)
- [9] J.S. Harrison, Z. Ounaies, 'Piezoelectric Polymers', NASA/CR-2001-211422, ICASE Report No. 2001-43 (2001)
- [10] http://www.airmar.com/piezoflex/piezo_index.html
- [11] W. J. Elspass, M. Flemming, 'Aktive Funktionsbauweisen', (Springer Verlag, Berlin Heidelberg New York, Germany, 1998)
- [12] <http://www.ndt.net/article/rocky/rocky.htm#2>
- [13] V. Sundar, Newnham, R. E., 'Electrostriction and polarization', Ferroelectrics, **135**, p. 431-446 (1992)
- [14] R. Kellogg, A. Flatau, 'Blocked force investigation of a Terfenol-D transducer', SPIE's 6th Annual International Symposium on Smart Structures and Materials, paper # 3668-19 (1999)
- [15] <http://www.txre.net/eng/xingneng.htm>
- [16] H. Jonocha, 'Application potential of magnetic field driven new actuators', 3rd European Conference on Magnetic Sensors and Actuators (EMSA), Dresden, Germany (2000)
- [17] F. Claeysen, N. Lhermet, T. Maillard, 'Magnetostrictive actuators compared to piezoelectric actuators', ASSET, European Workshop on Smart Structures in Engineering and Technology, France (2002)
- [18] K. Otsuka, C. M. Wayman 'Mechanism of shape memory effect and superelasticity', K. Otsuka, C. M. Wayman (eds), Shape memory materials, Cambridge University Press, Cambridge, pp. 27-48 (1998)
- [19] W. J. Buehler, R. C. Wiley, F. E. Wang, 'Nickel-Based Alloys', U. S. Patent 3,174,851,23, March 1965
- [20] H. Funakubo (Ed.), 'Shape Memory Alloys', (Gordon and Breach Science Publishers, New York, 1984)
- [21] http://www.memory-metalle.de/html/03_knowhow/PDF/MM_04_properties_e.pdf
- [22] <http://herkules.oulu.fi/isbn9514252217/html/x317.html>
- [23] K. Ullakko, 'Magnetically Controlled Shape Memory Alloys: A New Class of Actuator Materials', Journal of Material Engineering and Performance, Vol. **5**, 405-409 (1996)
- [24] R. O'Handley, S. Murray, M. Marioni, H. Nembach, S. Allen, 'Phenomenology of giant magnetic-field induced strain in ferromagnetic shape-memory materials' J. Appl. Phys., **87** (9), pp. 4712-4717, (2000)
- [25] J. Tellinen, I. Suorsa, A. Jääskeläinen, I. Aaltio and K. Ullakko, 'Basic properties of magnetic shape memory actuators' 8th international conference ACTUATOR 2002, Bremen, Germany, 10-12 June (2002)

- [26] I. Chopra, V. Kokorin, 'Magnetic-field induced twin boundary motion in magnetic shape-memory alloys' *Phys. Rev. B.*, 61 (66), pp. 4913–4915 (2000)
- [27] R. N. Couch, I. Chopra, 'Quasi-Static Modeling of NiMnGa Magnetic Shape Memory Alloy', *Proc. of SPIE Smart Structures and Materials: Active Materials – Behaviour and Mechanics*, 5387-84, pp. 528-541, San Diego, California, USA (2004)
- [28] W. C. Roentgen, 'About the changes in shape and volume of dielectrics caused by electricity', Section III in G. Wiedemann (Ed.), *Annual Physics and Chemistry Series*, Vol. 11, John Ambrosius Barth Publisher, Leipzig, Germany (1880)
- [29] Y. Bar-Cohen, 'Electroactive Polymer (EAP) - Actuators as Artificial Muscles - Reality, Potential, and Challenges', (SPIE Press, Bellingham, Washington, USA, 2004)
- [30] Q. M. Zhang, V. Barti, X. Zhao, 'Giant electrostriction and relaxor ferroelectric behaviour in electron-irradiated poly(vinylidene fluoride-trifluoroethylene) copolymer', *Science*, Vol. **280**, pp. 2101-2104 (1998)
- [31] F. Xia, Z.-Y. Cheng, H. Xu, H. Li, Q. M. Zhang, G. Kavarnos, R. Ting, G. Abdul-Sedat, K. D. Belfield, 'High electromechanical responses in a poly(vinylidene fluoride-trifluoroethylene-chlorofluoroethylene terpolymer)', *Adv. Mater.* **14**, 1574 (2002)
- [32] Z.-Y. Cheng, T.-B. Xu, V. Bharti, S. Wang, Q. M. Zhang, 'Transverse strain responses in the electrostrictive poly(vinylidene fluoride-trifluoroethylene) copolymer', *Appl. Phys. Lett* 74, 1901-1903 (1999)
- [33] Q. M. Zhang, H. Li, M. Poh, H. Xu, Z.-Y. Cheng, F. Xia, C. Huang, 'An all-organic composite actuator material with high dielectric constant', *Nature*, **419**, 284 (2002)
- [34] J. Su, J. S. Harrison, T. L. St. Clair, Y. Bar-Cohen, S. Leary, 'Electrostrictive graft elastomers and applications', *Mat. Res. Soc. Symp. Proc.* Vol. 600, Warrendale, PA, pp. 131-136 (1999)
- [35] <http://www.nusil.com/PDF/CF19-2186P.pdf>
- [36] <http://www.dowcorning.com/DataFiles/090007b580101a78.pdf>
- [37] 3M VHB 4910 Double coated Acrylic Foam Tapes:
<http://multimedia.mmm.com/mws/mediawebserver.dyn?8888882dpil8r0y8K0y888DgiIs0kX5b->
- [38] R. D. Kornbluh, D. S. Flamm, H. Prahlad, K. M. Nashold, S. Chhokar, R. Pelrine, D. L. Huestis, J. Simons, T. Cooper, D. G. Watters, 'Shape control of large lightweight mirrors with dielectric elastomer actuation', *Proc. of SPIE Smart Structures and Materials: Electroactive Polymers Actuators and Devices*, 5051, pp. 143-158 (2003)
- [39] K. Oguro, Y. Kawami, H. Takenaka, 'An actuator element of polyelectrolyte gel membrane-electrode composite', *Osaka Kogyo Gijutsu Shikensho Kiho*, 43, no. 1, pp. 21-24 (1992)
- [40] S. Nemat-Nasser, J. Y. Li, 'Electrochemical response of ionic polymermetal composites', *J. Applied Science*, Vol. 87, No. 7, pp. 3321-3331 (2000)

- [41] K. Asaka, K. Oguro, Y. Nishimura, M. Mizuhata, H. Takenaka, 'Bending of polyelectrolyte membrane-platinum composites by electric stimuli. Part 1. Response characteristics to various waveforms', *Polymer J.* vol. 27, no. 4, pp. 436-440 (1995)
- [42] Y. Bar-Cohen, S. Sherrit, Shyh-Shiuh Lih, 'Characterisation of Electromechanical Properties of EAP Materials', *Proc. of SPIE Smart Structures and Materials: Electroactive Polymers Actuators and Devices*, 4329-43, (2001)
- [43] S. Nemat-Nasser, 'Micromechanics of Actuation of Ionic Polymer-metal Composites', *J. Appl. Phys.*, vol. 92, no. 5, pp 2899-2915, (2002)
- [44] E. Smela, O. Inganäs, I. Lundström, Controlled folding of micrometer-size structures, *Science*, vol. 268, pp. 1735-1738 (1995)
- [45] T. F. Otero, H. Grande, J. Rodriguez, 'A new model for electrochemical oxidation of polypyrrole under conformational relaxation control', *J. Electroanal. Chem.*, vol. 394, pp. 211-216 (1995)
- [46] J. D. Madden, R. A. Cush, T. S. Kanigan, I. W. Hunter, 'Fast contracting polypyrrole actuators', *Synt. Met.* vol. 113, pp. 185-192 (2000)
- [47] J.-M. Sansinena, J. Gao, H.-L. Wang, 'High-Performance, Monolithic Polyaniline Electrochemical Actuators', *Advanced Functional Materials*, vol. 13, issue 9, pp. 703-709 (2003)
- [48] S. Iijima, 'Helical microtubes of graphitic carbon', *Nature*, vol. **345**, p56 (1991)
- [49] Gao, G.; T. Cagin, W. A. Goddard: 'Energetics, Structure, Mechanical and Vibrational Properties of Single Walled Carbon Nanotubes (SWNT)', the Fifth Foresight Conference on Molecular Nanotechnology, Nov. 5-8, Palo Alto, CA, USA (1997)
- [50] M. F. Yu, B. S. Files, S. Arepalli, R. S. Ruoff, 'Tensile loading of ropes of single wall carbon nanotubes and their mechanical properties', *Physical Review Letters*, **84**, 5552-5555 (2000)
- [51] D. A. Walters, L. M. Ericson, M. J. Casavant, J. Liu, D. T. Colbert, K. A. Smith, R. E. Smalley, 'Elastic strain of freely suspended single-wall carbon nano-tube ropes', *Appl. Phys. Lett.* **74**, 3803 (1999)
- [52] R. H. Baughman, C. Cui, A. A. Zakhidov, Z. Iqbal, J. N. Barisci, G. M. Spinks, G. G. Wallace, A. Mazzoldi, D. De Rossi, A. G. Rinzler, O. Jaschinski, S. Roth, M. Kertesz, 'Carbon nanotube actuators', *Science*, vol. **284**, pp. 1340-1344 (1999)
- [53] R. H. Baughman, A. A. Zakhidov, W. A. de Heer, 'Carbon Nanotubes - the Route Toward Applications', *Science*, vol. 297, pp. 787-792 (2002)
- [54] Roux, J., 'High performance and multifunctional carbon nanotubes based materials', *Micro / Nanotechnologies for Space*, ESA-ESTEC, Noordwijk, 20-22 May (2003)
- [55] A. B. Dalton, S. Collins, E. Munoz, J. M. Razal, V. H. Ebron, J. P. Ferraris, J. N. Coleman, B. G. Kim, R. H. Baughman, 'Super-tough carbon-nanotube fibres', *Nature*, **423**, p. 703 (2003)